Applied Catalysis B: Environmental 197 (2016) 236–243

Contents lists available at ScienceDirect

Applied Catalysis B: Environmental

journal homepage: www.elsevier.com/locate/apcatb

On the effect of Ce incorporation on pillared clay-supported Pt and Ir catalysts for aqueous-phase hydrodechlorination

A.H. Pizarro[a,*], C.B. Molina[a], J.L.G. Fierro[b], J.J. Rodriguez[a]

[a] Chemical Engineering Area, Faculty of Sciences, Universidad Autónoma de Madrid, Cantoblanco, 28049 Madrid, Spain
[b] Instituto de Catálisis y Petroleoquímica (CSIC), Cantoblanco, 28049 Madrid, Spain

ARTICLE INFO

Article history:
Received 29 November 2015
Received in revised form 22 February 2016
Accepted 25 February 2016
Available online 2 March 2016

Keywords:
Hydrodechlorination
Hydrodenitrogenation
Chlorophenol
Chloroaniline
Pt
Ir
Ce
Pillared clays

ABSTRACT

Hydrodechlorination (HDC) of chlorinated pollutants in water such as 4-chlorophenol (4-CP) and 4-chloroaniline (4-CA) was carried out with catalysts based on Pt and Ir supported pillared clays. Almost complete dechlorination was achieved at short reaction time under mild operation conditions with the Pt catalyst. The incorporation of cerium oxide to the Pt and Ir catalysts (PtCe and IrCe catalysts, respectively) led to a higher dispersion than that of the monometallic ones. The catalyst loaded with Pt showed low reaction rates and conversion while the one modified with increasing amounts of cerium oxide was highly active for conversion of the chlorinated pollutants. On the contrary, the IrCe catalysts were found poorly active due to partial coverage of Ir crystallites by cerium oxide.

1. Introduction

The removal of chlorinated organic compounds represents one of the priorities in water treatment due to their harmful effects and the new and more restrictive environmental legislation. Chlorinated and chloronitrogenated aromatic compounds such as chlorophenols and chloroanilines are usually classified as harmfull or toxic agents [1] that can cause cancer [2] and other harmful effects. Nevertheless, these molecules are widely used in the production of pesticides, antioxidants, dyes or other chemicals. Chlorophenols have been regarded as useful industrial products with a broad range of applications, being used as versatile anti-microbial and disinfecting agents, fungicides, insecticides, algicides, herbicides and as synthetic precursors for a variety of pharmaceuticals, glues, paints, dyestuffs and inks. Chlorinated anilines are harmful pollutants, forbidden in some countries for their carcinogenic effects and their high toxicity [3]. The European Union (EU) restricted some azo-dyes in textile industry due to possible formation of this kind of compounds (EU 2002/61/CE and Regulation 1907/2006, REACH directive). The 4-chloroaniline (4-CA) is used in the production of pesticides, approved by the EU for use such as pyraclostrobin and diflubenzuron, different drugs, dyes and biocides widely used in healthcare products like chlorhexidine or triclocarban.

Catalytic HDC has been investigated during the last decades being very effective in the elimination of chlorinated pollutants in aqueous phase such as chlorophenols with H_2 [4–7] or formic acid [8,9] as reducing agents, pesticides [10–14] or chloronitrogenated pollutants [15], diminishing the toxicity of the effluents containing these compounds.

Cerium oxide catalysts are commonly used in fuel cells, solar cells and three-way catalysts [16,17]. Nanostructured CeO_2 materials generally improve the properties compared to microsized or bulk materials [18]. The ability to store oxygen under oxidizing conditions and release it under reducing conditions makes these materials ideal for several environmental applications. Cerium oxide has been also used in the synthesis of precious metal catalysts to prevent the sinterization of metallic nanoparticles, increasing the catalyst dispersion [19], as it has been demonstrated when incorporating cerium oxide to Pt/Al_2O_3 [20], $Rh\text{-}Mo/ZrO_2$ [21] and Al-PILC catalysts supporting Pd [22,23], Pt [24] or transition metals such as Mn [25]. On the other hand, CeO_2 can be used to increase the stability of some catalysts [25]. It has been also used in the synthesis of pillared clays with Fe for phenol oxidation in aqueous phase, improving its catalytic activity [26,27].

* Corresponding author.
E-mail address: alejandro.herreropizarro@gmail.com (A.H. Pizarro).

http://dx.doi.org/10.1016/j.apcatb.2016.02.056
0926-3373/

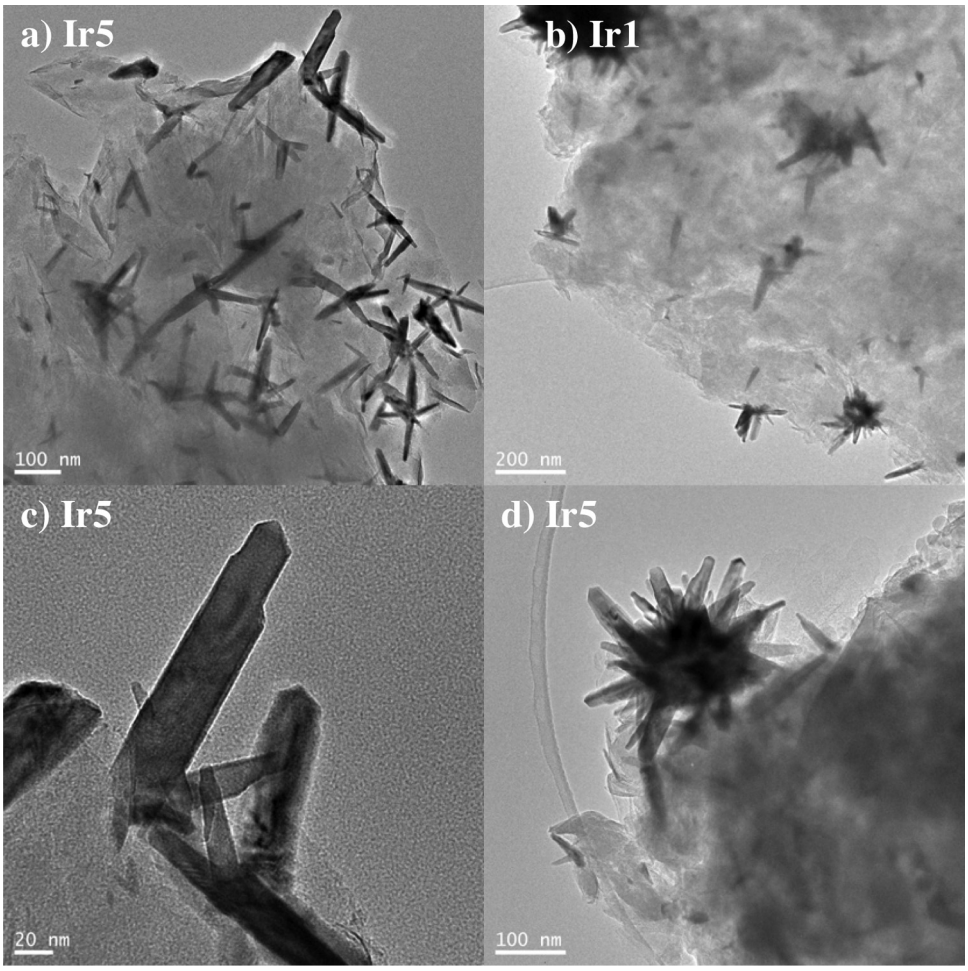

Fig. 1. TEM images of Ir1 (b) and Ir5 (a, c, d) at different scales.

The Pt and Ir catalysts have been less studied for HDC than those of Pd and Rh and they have shown less activity and a faster deactivation [7,28]. Nevertheless, the activity can be improved with the addition of promoters or other metals that allow a higher dispersion of the active phase avoiding the nucleation and growth of the nanoparticles over the support. The strong metal-CeO_2 interactions favour a higher metal dispersion compared to other supports [29–32]. In line with above, this work was undertaken with the aim to study the aqueous phase HDC of 4-CP on Pt and Ir catalysts and the HDC/HDN of 4-CA on PtCe catalyst focusing on the effect of Ce incorporation on their catalytic performance.

2. Materials and methods

2.1. Pillared clays preparation

The Pt catalyst was prepared using an Al-pillared clay (Al-PILC) as support. The starting material used in its preparation was a purified-grade bentonite supplied by Fisher Scientific Company (Loughborough, Oregon, USA). The chemical analysis (wt%) of this bentonite was: SiO_2, 52.22; Al_2O_3, 16.81; Fe_2O_3, 3.84; Na_2O, 1.26; MgO, 0.88; CaO, 0.74; K_2O, 0.80. Briefly, an aluminium pillaring solution was prepared (OH/Al = 2 molar ratio) and added to a bentonite suspension (1 wt%) providing 10 mmol of Al per gram of clay. The resulting material was washed by centrifugation with deionized water, dried overnight at 110 °C and calcined at 350 °C for 2 h. The cation-exchange capacity (CEC) was 97 meq per 100 g of clay. Al-PILC was obtained following the method described elsewhere [9].

The monometallic Pt and Ir catalysts were prepared by wet impregnation of Al-PILC using a solution of H_2PtCl_6 (8%wt) or $IrCl_3{\cdot}H_2O$. The bimetallic PtCe and IrCe catalysts were prepared by co-impregnation of H_2PtCl_6 or $IrCl_2{\cdot}H_2O$ and $Ce(NO_3){\cdot}6H_2O$, dissolved in an aqueous solution of HCl (1 M). These solutions were impregnated on 1 g of Al-PILC prior to calcination. The impregnated solid was dried at room temperature for 2 h, then at 110 °C for 14 h and, finally, calcined for 2 h at 500 °C. The resulting Pt, Ir, PtCe and IrCe catalysts, were loaded with 1 wt% in the case of Pt, 1 or 5 wt% of Ir and 3, 5 or 10 wt% of Ce(x) are referred to hereafter as Pt1, Ir1, Ir5 and Pt1Cex or Ir1Cex, respectively.

2.2. Catalyst characterization methods

A Micromeritics Tristar 3000 apparatus was used to obtain the N_2 adsorption-desorption isotherms at −196 °C. The samples were previously degassed at 160 °C and 5×10^{-3} Torr for 16 h. Specific areas were obtained according to Brunauer–Emmet–Teller (BET) method. The Pt, Ir and Ce loadings of the catalysts were determined by inductively coupled plasma mass spectroscopy (ICP-MS) by means of a Model Elan 6000 Sciex PerkinElmer apparatus. The particle size distribution of the metallic phase was determined by transmission electron microscopy (TEM) using a JEOL 2100F microscope with a point resolution of 0.19 nm coupled with an energy-dispersive X-ray spectrometer (EDXS; INCA x-sight, Oxford

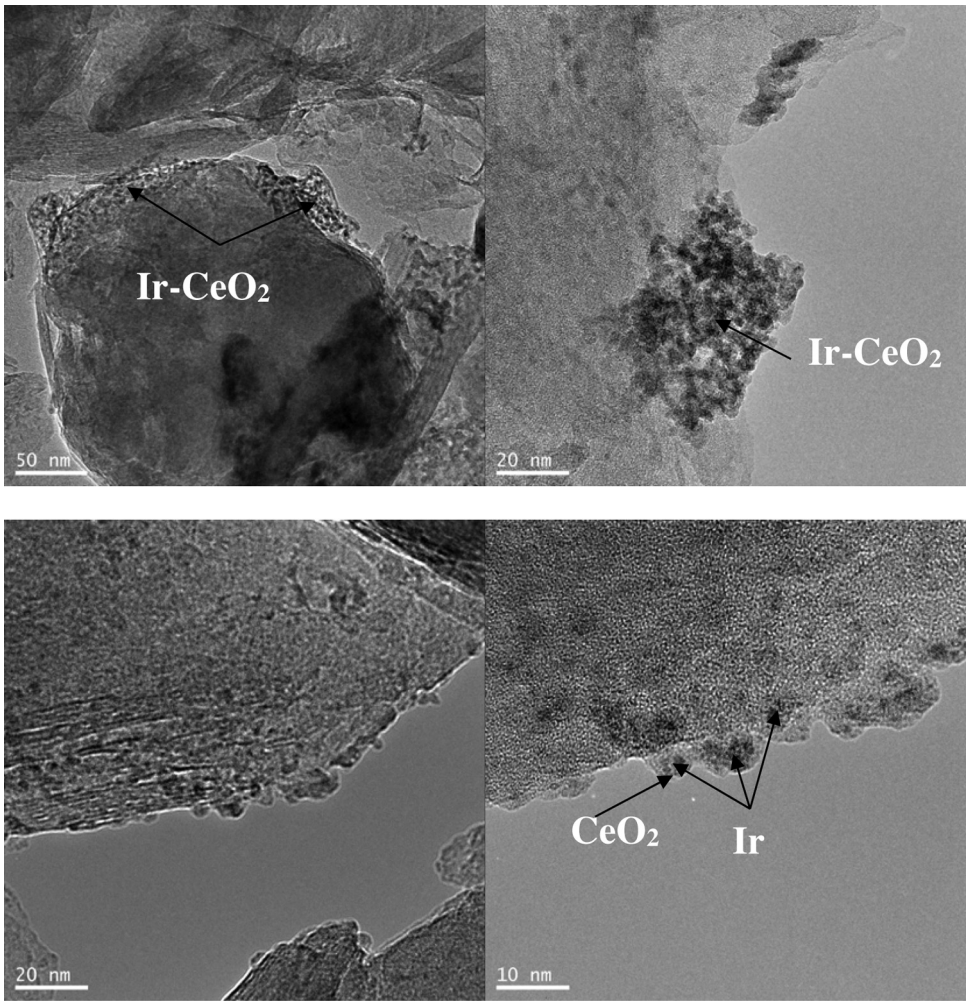

Fig. 2. TEM images of Ir1Ce10 at different scales.

Instruments) used for elemental analysis. The chemical state of the elements and relative dispersion of active phases was obtained by X-ray photoelectron spectroscopy (XPS). Photoelectron spectra were recorded by means of a VG Escalab 200R spectrometer, provided with MgKα ($h\nu = 1253.6$ eV) X-ray source. The peaks were fitted by a non-linear least square fitting routine using a properly weighted sum of Lorentzian and Gaussian component curves after background subtraction according to Shirley. The atomic ratios of the elements on the surface were calculated from the integrated peaks areas normalized by atomic sensitivity factors. Prior to analysis, all catalyst samples were pre-reduced at various temperatures.

2.3. HDC and HDC/HDN measurements

The catalytic activity measurements were performed in a batch glass reactor of 1.1 L of capacity at 25 °C and atmospheric pressure using H_2 as hydrogenating agent, 1 g/L of catalyst and 1 L with a concentration of 100 mg/L of 4-chlorophenol or 4-chloroaniline using magnetic stirring (360 rpm). All the catalysts were dried overnight at 120 °C before the reduction step. This previous reduction step was developed for 2 h at 90 °C inside a packed fixed-bed reactor (Pyrex glass, 30 cm length, 9 mm inner diameter) under a H_2 flow of 35 NmL/min, conditions selected in a previous work [28]. Also reduction temperatures of 200 and 400 °C were used to test the

Table 1
Characterization of the starting material and the catalysts tested.

Catalyst	BET Surface area (m^2/g)	External area (m^2/g)	Micropore volume (cm^3/g)	Mean Pore size (nm)	Pt or Ir content (%)	Ce content (%)
Al-PILC	212	69	0.059	3.5		
Pt1	178	66	0.056	3.8	1.02	
Ir1	146	54	0.042	4.4	0.98	
Ir5	114	39	0.034	4.1	5.41	
Ir1Ce3	88	37	0.024	4.4	0.98	3.41
Ir1Ce5	85	35	0.022	4.0	0.97	5.54
Ir1Ce10	63	29	0.018	3.8	0.95	9.55
Pt1Ce3	123	38	0.039	4.0	0.98	2.85
Pt1Ce5	122	35	0.041	4.0	1.01	5.79
Pt1Ce10	114	33	0.038	4.0	0.99	9.60

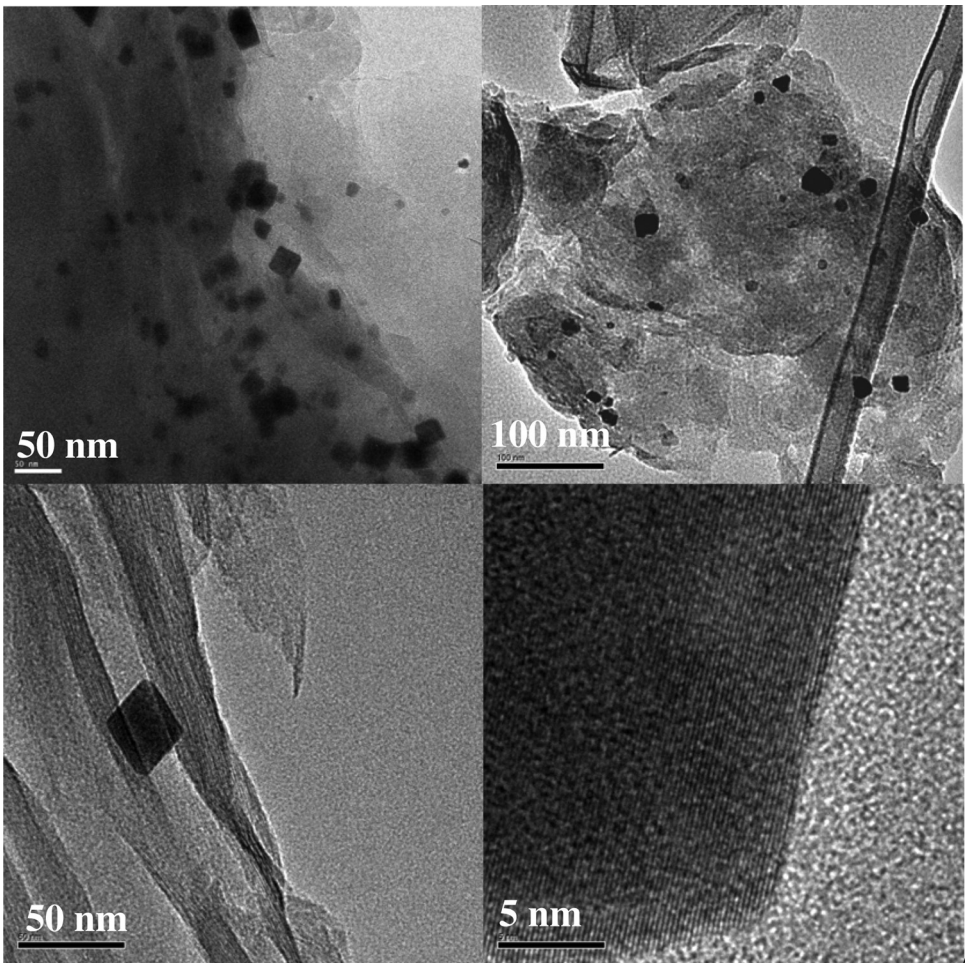

Fig. 3. TEM images of Pt1 at different scales.

influence of this variable in the XPS analyses (see below). After reduction, the gas in the fixed-bed reactor was purged using a N_2 flow of 35 NmL/min for 30 min.

Next, the catalyst was introduced into the batch glass reactor and stirring was maintained for 15 min. Then, hydrogen was fed to the reactor at a continuous flow rate of 50 NmL/min. Samples were withdrawn from the reactor at 5, 10, 15, 30 min and each hour until the end of the experiment. The catalyst was separated by filtration using 0.45 μm pore size PTFE filters. Internal and external mass transfer limitations were discarded in our working conditions as confirmed by several preliminary experiments where the effect of stirring speed and particle size were checked.

2.4. Analytical methods

4-CP, 4-CA, phenol and aniline concentrations were measured by HPLC with an UV detector using a C18 column as stationary phase at 210 nm, and as mobile phase a mixture acetonitrile-water (4-CP, phenol) or methanol-water (4-CA, aniline) (1:1 v/v, flow 1 mL/min). 4-CP, 4-CA and aniline were also analyzed and quantified, as well as cyclohexanone and cyclohexanol, by means of a GC/FID using a CP-Wax 52CB, Varian (30 m length and 0.25 mm i.d.) capillary column.

The metal content in the HDC effluents was measured by total-reflection X-ray fluorescence with a TXRF EXTRA-II (Rich & Seifert, Germany).

3. Results and discussion

HDC of 4-CP is a very well known reaction involving several steps such as the scission of the C—Cl bond in addition to the hydrogenation of the aromatic ring, yielding phenol, cyclohexadienol, cyclohexenol, cyclohexanone and cyclohexanol under ambient-like conditions. It has been reported that Pt catalysts, as well as the Rh ones, are able to promote the hydrogenation of phenol to a higher extent than Pd ones giving rise to the formation of cyclohexanol [7]. Moreover, pillared clay-supported Pd catalysts yield cyclohexanone as final reaction product. The HDC/HDN pathways of 4-CA involve the scission of the C—Cl bond to aniline and a subsequent reductive hydrolysis on the latter, yielding cyclohexanone as main reaction product [15].

3.1. Characterization of mono and bimetallic catalysts

Table 1 shows the characterization of the porous structure as well as the metal loads of the mono and bimetallic Pt-PILC and Ir-PILC catalysts, with different cerium oxide loadings. Incorporation of increasing amounts of Ce to catalyst formulation results in a decrease in the specific BET surface area and the micropore volume as already observed with other bimetallic Al-pillared clay-based catalysts prepared in a similar manner [33,34]. IrCe catalysts showed a higher decrease in both BET area and micropore volume than the PtCe catalysts.

Figs. 1 and 2 show the morphology obtained by TEM analyses of the monometallic Ir1 and Ir5 catalysts and of the bimetallic Ir1Ce10

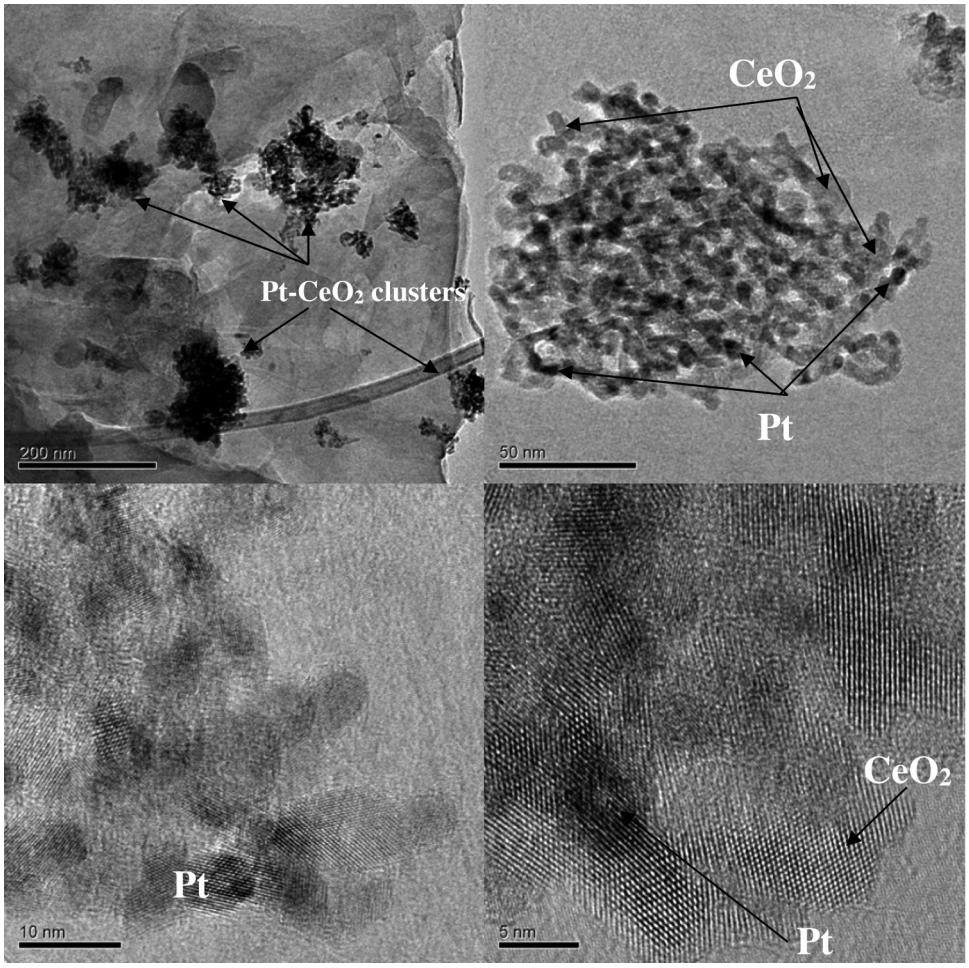

Fig. 4. TEM images of Pt1Ce10 at different scales.

ones, respectively. It can be noted that the monometallic Ir5 catalysts shows crystallites with acicular morphology homogeneously distributed over the surface, with sizes between 20–150 nm, while the Ir1 one presents less crystallites of similar morphology but of lower size. The bimetallic Ir1Ce10 catalysts showed similar appearance than the PtCe ones (see below), with nanoparticles of Ir lower than 5 nm, mixed homogeneously with the CeO_2 phase. It is emphasized that some Ir crystallites appear immersed in a matrix of cerium oxide or covered by very thin layer of this oxide as probed with the EDX analysis in the TEM study (Fig. 2).

Figs. 3 and 4 show some TEM micrographs belonging to the mono and bimetallic catalysts Pt1 and Pt1Ce10, respectively, at different scales. The monometallic catalyst shows Pt crystallites with sizes in the range 5–30 nm. The PtCe catalysts, however, display metallic crystallites with sizes below 5 nm and surrounded by Ce particles which probes the higher dispersion of Pt achieved in the PtCe catalysts. This agrees with XPS data showed in Table 2 (see below).

3.2. HDC of 4-CP with IrCe catalysts

Fig. 5 shows the HDC of 4-CP on the Ir1 monometallic catalyst. This catalyst allowed around 70% conversion of 4-CP after 4 h reaction time under the ambient-like conditions tested. The evolution of reactant and products follows a similar trend than that observed in the HDC of 4-CP on Pt or Rh catalysts supported on Al-PILCs [7], which yielded phenol, cyclohexanone and cyclohexanol as final products (Fig. 5).

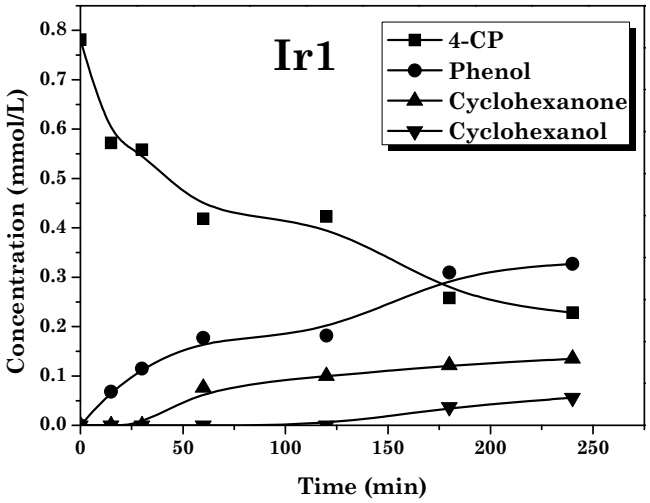

Fig. 5. HDC of 4-CP with Ir1 catalyst (25 °C, 1 atm, pH 6, $[catalyst]_0$ = 1 g/L, $[4\text{-}CP]_0$ = 0.77 mmol/L (100 mg/L), Q_{H2} = 50 NmL/min).

Similarly, the bimetallic IrCe catalysts containing variable amounts of Ce were also tested in the HDC of 4-CP (Fig. 6). A general trend observed is that the catalytic activity drops when increasing Ce loading, and especially for the catalyst with the highest Ce loading (Ir1Ce10). In addition, selectivities to cyclohexanone and cyclohexanol also decreased upon increasing Ce loading. This

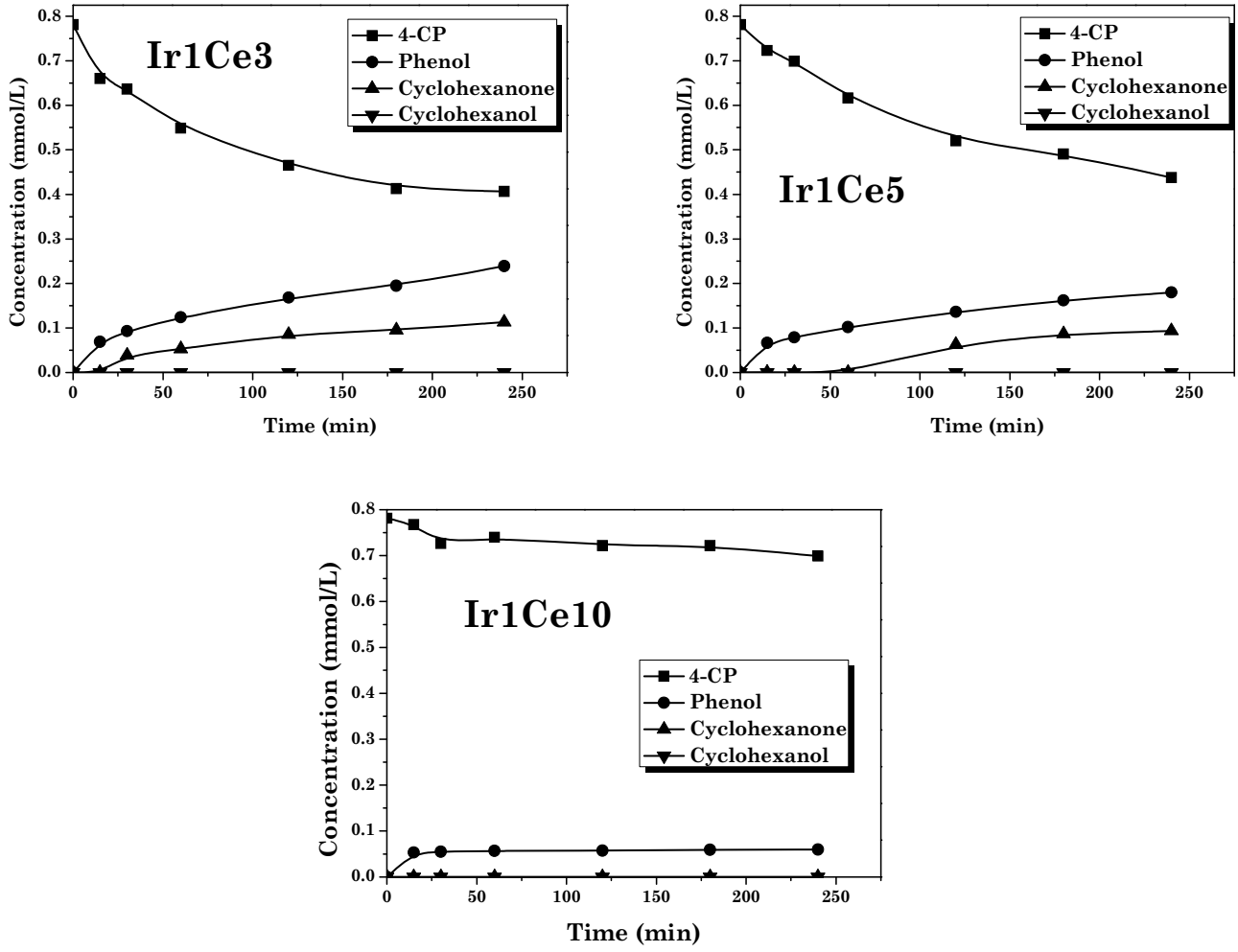

Fig. 6. HDC of 4-CP with IrCe catalysts (25 °C, 1 atm, pH 6, $[catalyst]_0$ = 1 g/L, $[4\text{-CP}]_0$ = 0.77 mmol/L (100 mg/L), Q_{H2} = 50 NmL/min).

behaviour can be explained in terms of the strong interaction of Ir crystallites on the surface of CeO_2, or even by the partial coverage of Ir crystallites by a thin layer of CeO_2. The relative ease with which cerium oxide interacts, or covers Ir crystallites leads to a decrease of the catalytic activity. From TEM images shown in Fig. 2 it is apparent that CeO_2 placed on the metal surface might well limit the access of the reactant molecules to the metal surface. TXRF analyses of the HDC effluents showed absence of metal leaching, thus indicating good stability of the catalyst.

3.3. HDC of 4-CP and 4-CA with PtCe catalysts

The bimetallic PtCe catalysts tested in the HDC of 4-CP displayed a different behaviour. Fig. 7 shows the conversion of 4-CP on Pt catalysts containing variable amounts of CeO_2. All the bimetallic PtCe catalysts showed higher catalytic activity than the monometallic one (initial rate of 0.42 mmol/min g_{Pt}). The catalyst Pt1Ce5 yielded the highest 4-CP conversion and initial reaction rate (1.6 mmol/min g_{Pt}) with almost a complete conversion of 4-CP after 4 h of reaction. Similarly, the catalyst Pt1Ce3 displayed essentially the same catalytic behaviour than the Pt1Ce5 one. However, the activity of the catalyst with the highest Ce loading (Pt1Ce10) started to decline probably because of the excess of Ce used which accumulates in the pores and covers to a some extent Pt crystallites. It is emphasized that the carbon balance matched between 95 and 100% and an almost total completely for chlorine was achieved in all the experiments.

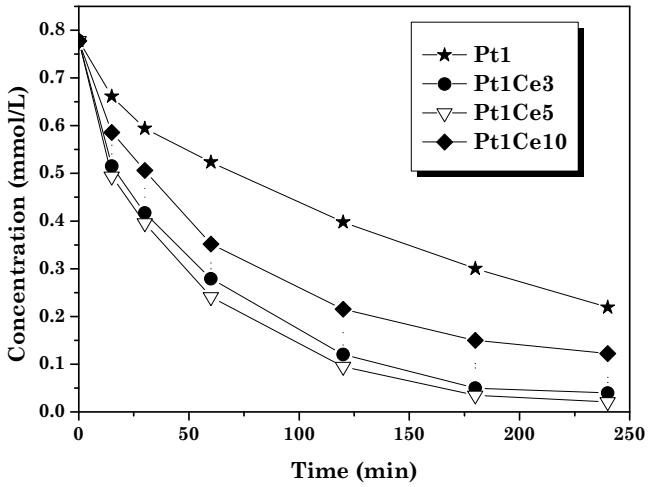

Fig. 7. Conversion of 4-CP with Pt1 and Pt1Ce5 catalysts (25 °C, 1 atm, pH 6, $[catalyst]_0$ = 1 g/L, $[4\text{-CP}]_0$ = 0.77 mmol/L (100 mg/L), Q_{H2} = 50 NmL/min).

Fig. 8 represents the results obtained on the HDC of 4-CP on Pt1 and Pt1Ce5 catalysts. As can be seen, the bimetallic catalyst allowed complete conversion of phenol into cyclohexanone and cyclohexanol. Contrary to the results obtained with Ir1Cex catalysts, in Pt catalysts the Ce oxide does not cover the Pt crystallites but produces some agglomerations of Pt and CeO_2. A previous work

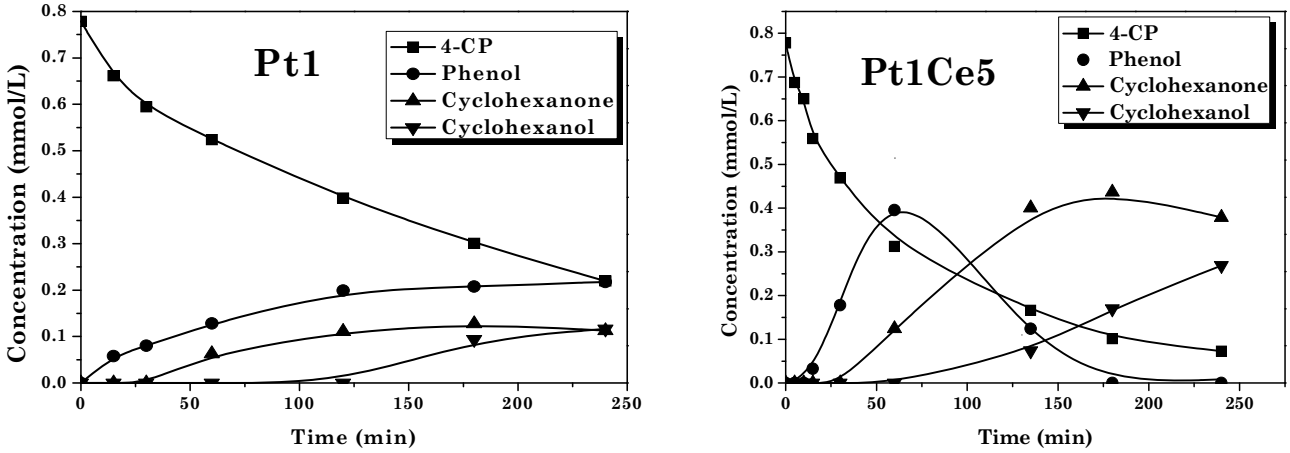

Fig. 8. HDC of 4-CP with Pt1 and Pt1Ce5 catalysts (25 °C, 1 atm, pH 6, $[catalyst]_0$ = 1 g/L, $[4\text{-CP}]_0$ = 0.77 mmol/L (100 mg/L), Q_{H2} = 50 NmL/min).

Table 2
Relative occurrence of metallic species in Pt1 and Pt1Ce10 reduced at different temperatures by XPS analyses.

Reduction T (H_2)	Pt1 $Pt^{\circ}/(Pt^{\circ}+Pt^{n+})$ (%)	Pt1Ce10 $Pt^{\circ}/(Pt^{\circ}+Pt^{n+})$ (%)
No reduction	43	48
90 °C	67	79
200 °C	100	100
400 °C	100	100

compared Pt/γ-Al_2O_3 and PtCe/γ-Al_2O_3 catalysts for the wet oxidation of phenol [20]. These catalysts were prepared by successive incipient wetness impregnation of Ce and Pt using $Ce(NO_3)_3$ and an anionic (H_2PtCl_6) or cationic ($Pt(NH_3)_4Cl_2$) precursor. The activity of the catalysts prepared with cerium oxide and the anionic Pt salt was lower than that obtained with the monometallic Pt catalyst while those bimetallic catalysts prepared with the cationic Pt precursor showed a remarkable increase of the catalytic activity. By contrast, the results shown herein demonstrate that the use of an anionic Pt precursor co-impregnated with Ce can improve the dispersion and the catalytic activity for the HDC. The same effect has been observed with Pd-containing pillared clays, which showed a better dispersion of Pd on an Al-Ce-PILC as compared to its cerium oxide-free Al-PILC substrate [22,35].

In order to obtain a deeper knowledge of the state of Pt and Ce in the catalysts XPS analyses were performed. The surface of the catalyst with the highest Ce loading (Pt1Ce10) and its Ce-free (Pt1) was analyzed. Moreover, the effect of the catalyst reduction temperature was also studied.

As the PILC substrate contains aluminium and hence the Al2p emission strongly overlaps with Pt4f levels, the $Pt4d_{5/2}$ core level spectra were recorded. The $Pt4d_{5/2}$ peak of Pt1 catalyst exhibited two components centered at binding energies of 315.0 and 317.0 eV, which correspond to Pt° metallic and Pt^{2+} species, respectively. The surface Pt species detected for Pt-1 and Pt1Ce10 catalysts at different reduction temperatures are collected in Table 2. It can be seen that the extent of reduced platinum in the binary Pt1Ce10 catalyst increases from 43% to 48% upon cerium oxide incorporation. It is also observed that if reduction temperature is 90 °C the proportion of zerovalent Pt increases up to 67% for catalyst Pt1 and a little more up to 79% in Pt1Ce10 one. The larger extent of Pt reduction in the Ce-loaded catalyst can be due to the higher dispersion of platinum in the binary system. It can also be noted that reduction temperature up to 200 °C leads to a complete reduction of the active phase into zerovalent platinum in both Pt1 and Pt1Ce10 catalysts. Moreover, the Ce3d spectrum reveals the appearance of a certain proportion of Ce^{3+} species indicating that the surface layer of CeO_2 became partially reduced. As this temperature is relatively low, it is likely that its reduction could be enhanced by the H-spillover generated at the metallic Pt crystallites.

As it can be seen in Table 3, incorporation of 10 wt% of Ce in the catalyst results in a higher Pt/Si atomic ratio than in the monometallic catalyst. This indicates that Pt dispersion of Pt1Ce10 is substantially higher than on its Pt1 counterpart (Pt dispersion of Pt1 is 10.8% [7]), indicating a higher Pt exposure to reactants. It is also observed that the Pt/Si ratio diminished with the increase of the reduction temperature in the case of the bimetallic Pt1Ce10 catalyst due to sinterization of Pt crystallites and/or to segregation of Cerium oxide. Although Pt sintering induced by reduction temperature is very likely, it might well occur because the drop of Pt exposure (Pt/Si ratio) runs in parallel with the increase of Ce/Si ratios, Table 3. Finally, it is emphasized that Fe/Si ratio remained essentially unchanged as a function of the reduction temperature. This is due to the fact that Fe^{3+} ions remain strongly linked to the silicate structure of the clay and hence it is neither reduced nor extracted from the lattice in the course of reduction treatments.

The HDC reaction of 4-CA on catalyst Pt1Ce5 was also investigated under the same operation conditions (Fig. 9). Complete conversion of 4-CA was attained at 1 h reaction time on stream. The initial rate in this case (2.78 mmol/min g_{Pt}) is remarkably faster than that observed for 4-CP HDC and similar than the one recorded for 4-CA HDC on the monometallic Pd-PILC catalyst [15] under the same experimental conditions. The differences in the surface

Table 3
Relative proportion of Fe, Pt and Ce by XPS analyses. Pt° relative occurrence in the catalysts reduced at different temperatures.

Catalyst	Fe/Si	Pt/Si ratio	Decrease of surface Pt (%)	Ce/Si ratio	Increase of surface Ce (%)
Pt1	–	0.0041	–	–	–
Pt1 90 °C	–	0.0042	–	–	–
Pt1Ce10	0.032	0.0082	–	0.064	–
Pt1Ce10 90 °C	0.033	0.0065	21	0.083	23
Pt1Ce10 200 °C	0.036	0.0057	31	0.097	35
Pt1Ce10 400 °C	0.030	0.0053	36	0.108	41

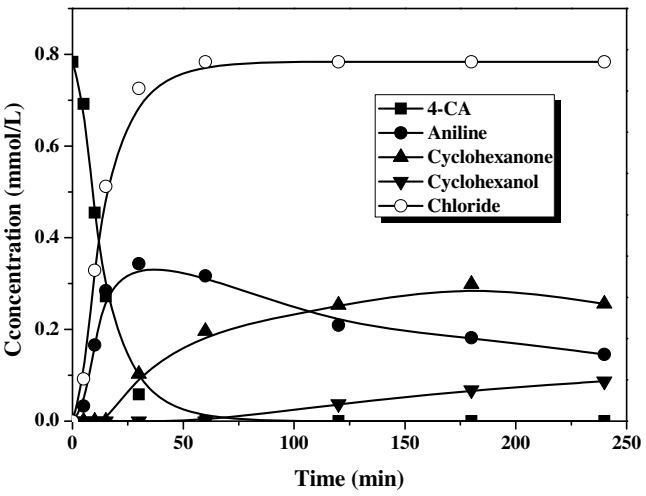

Fig. 9. HDC/HDN of 4-CA with Pt1Ce5 catalyst (25 °C, 1 atm, pH 6, $[catalyst]_0$ = 1 g/L, $[4\text{-CA}]_0$ = 0.78 mmol/L (100 mg/L), Q_{H2} = 50 NmL/min).

adsorption strength and in the mesomeric and inductive effects of the substituents determine the higher initial rate observed in the HDC of 4-CA compared with that of 4-CP, as it was previously reported by Aramendia et al. (2003) using methanol as solvent [36]. In this reaction, the main intermediate observed after the dechlorination was aniline which evolved to cyclohexanone through reductive hydrolysis. Cyclohexanol was obtained as final product following the same reaction pathways as for phenol hydrogenation with Pt catalysts. The chlorine balance was completely closed in this reaction but the carbon balance was closed only at a 62% indicating the existence of some unidentified by-products in the solution and/or species adsorbed onto the catalyst surface. The limiting steps in both processes are the hydrogenation of phenol to cyclohexanone and the hydrolysis of aniline to cyclohexanone. It is emphasized that these reaction products resulting from the catalytic hydrotreatment of 4-CP and 4-CA are by far less ecotoxic than the starting compounds [4,37–40]. TXRF analyses of the effluents from the HDC of 4-CP and 4-CA demonstrated absence of Pt leaching under the reaction conditions used in this work.

4. Conclusions

The effect of CeO_2 incorporation into Pt and Ir catalysts supported on Al-PILC was studied in the aqueous-phase HDC of 4-CP and HDC/HDN of 4-CA. The results obtained showed the positive effect of CeO_2 incorporation by co-impregnation to Pt, but opposite when it was incorporated to Ir catalyst. The strong interaction of CeO_2 with the noble metals seems to be responsible for the high metallic dispersion in the bimetallic catalysts synthesised in this work. A remarkable increase in Pt and Ir dispersion was observed in bimetallic catalysts compared with monometallic ones.

The interaction of CeO_2 with Ir avoids the access of reactants to the Ir active sites, thus diminishing the catalytic activity upon CeO_2 incorporation. However, the simultaneous incorporation of both Pt and CeO_2 resulted in a higher catalytic activity in the HDC of 4-CP with respect to the monometallic Pt catalyst. The HDC/HDN of 4-CA on the catalyst Pt1Ce5 resulted in a high dechlorination rate and the production of cyclohexanone and cyclohexanol as the main final reaction products.

Acknowledgments

The authors want to thank financial support from the Spanish Plan Nacional de I+D+ithrough the project CTQ2013-41963-R.

References

[1] V. Aruoja, M. Sihtmäe, H. Dubourguier, A. Kahru, Chemosphere 84 (2011) 1310–1320.
[2] C.R. Jones, L. Yu-Yin, O. Sepai, H. Yan, G. Sabbioni, Environ. Sci. Technol. 40 (2006) 387–394.
[3] R.S. Chhabra, J.E. Huff, J.K. Haseman, M.R. Elwell, A.C. Peters, Food. Chem. Toxicol. 29 (1991) 119–124.
[4] L. Calvo, A.F. Mohedano, J.A. Casas, M.A. Gilarranz, J.J. Rodriguez, Carbon. 42 (2004) 1377–1381.
[5] G. Yuan, M.A. Keane, Catal. Commun. 4 (2003) 195–201.
[6] E. Diaz, J.A. Casas, A.F. Mohedano, L. Calvo, M.A. Gilarranz, J.J. Rodriguez, Ind. Eng. Chem. Res. 48 (2009) 3351–3358.
[7] C.B. Molina, A.H. Pizarro, J.A. Casas, J.J. Rodriguez, Appl. Catal. B: Environ. 148–149 (2014) 330–338.
[8] C.B. Molina, L. Calvo, M.A. Gilarranz, J.A. Casas, J.J. Rodriguez, Appl. Clay. Sci. 45 (2009) 206–212.
[9] C.B. Molina, L. Calvo, M.A. Gilarranz, J.A. Casas, J.J. Rodriguez, J. Hazard. Mater. 172 (2009) 214–223.
[10] L. Calvo, M.A. Gilarranz, J.A. Casas, A.F. Mohedano, J.J. Rodriguez, Appl. Catal. B: Environ. 78 (2008) 259–266.
[11] M. Al Bahri, L. Calvo, A.M. Polo, M.A. Gilarranz, A.F. Mohedano, J.J. Rodriguez, Chemosphere 91 (2013) 1317–1323.
[12] C. Schüth, M. Reinhard, Appl. Catal. B: Environ. 18 (1998) 215–221.
[13] S.S. Zinovyev, N.A. Shinkova, A. Perosa, P. Tundo, Appl. Catal. B: Environ. 47 (2004) 27–36.
[14] S. Ordoñez, E. Díaz, R.F. Bueres, E. Asedegbega, H. Sastre, J. Catal. 272 (2010) 158–168.
[15] A.H. Pizarro, C.B. Molina, J.A. Casas, J.J. Rodriguez, Appl. Catal. B: Environ. 158–159 (2014) 175–181.
[16] S.Y. Christou, S. García-Rodríguez, J.L.G. Fierro, A.M. Efstathiou, Appl. Catal. B: Environ. 111–112 (2012) 233–245.
[17] H.S. Gandhi, G.W. Graham, R.W. McCabe, J. Catal. 216 (2003) 433–442.
[18] J. Xu, J. Harmer, G. Li, T. Chapman, P. Collier, S. Longworthb, S.C. Tsang, Chem. Commun. 46 (2010) 1887–1889.
[19] P.O. Thevenin, A. Alcalde, L.J. Pettersson, S.G. Järås, J.L.G. Fierro, J. Catal. 215 (2003) 78–86.
[20] S.K. Kim, S.K. Ihm, Ind. Eng. Chem. Res. 41 (2002) 1967–1972.
[21] P. Reyes, I. Concha, G. Pecchi, J.L.G. Fierro, J. Mol. Catal. A: Chem. 129 (1998) 269–278.
[22] S. Zuo, R. Zhou, App. Surf. Sci. 253 (2006) 2508–2514.
[23] S. Zuo, Q. Huang, R. Zhou, Catal. Today 139 (2008) 88–93.
[24] M. Barrera-Vargas, O.A. Almanza, J.C. Carriazo, Scientia et Technica Año XIII (2007) 489–493.
[25] S. Zuo, Q. Huang, J. Li, R. Zhou, Appl. Catal. B: Environ. 91 (2009) 204–209.
[26] A. Olaya, G. Blanco, S. Bernal, S. Moreno, R. Molina, Appl. Catal. B: Environ. 93 (2009) 56–65.
[27] N.R. Sanabria, M.A. Centeno, R. Molina, S. Moreno, Appl. Catal. A: Gen. 356 (2009) 243–249.
[28] C.B. Molina, A.H. Pizarro, M.A. Gilarranz, J.A. Casas, J.J. Rodriguez, Chem. Eng. J. 160 (2010) 578–585.
[29] W. Lin, A.A. Herzing, C.J. Kiely, I.E. Wachs, J. Phys. Chem. C 112 (2008) 59425951.
[30] N. Barrabés, K. Föttinger, A. Dafinov, F. Medina, G. Rupprechter, J. Llorca, J.E. Sueiras, Appl. Catal. B: Environ. 87 (2009) 84–91.
[31] D.R. Ou, T. Mori, H. Togasaki, M. Takahasi, F. Ye, J. Drenan, Langmuir 27 (7) (2011) 3859–3866.
[32] A. Bruix, J.A. Rodriguez, P.J. Rodriguez, S.D. Senanayake, J. Evans, J.B. Park, D. Stacchiola, P. Liu, J. Hrbek, F. Illas, J. Am. Chem. Soc. 134 (2012) 8968.
[33] C.B. Molina, A.H. Pizarro, J.A. Casas, J.J. Rodriguez, Water Sci. Technol. 65 (2012) 653.
[34] A.H. Pizarro, C.B. Molina, J.J. Rodriguez, F. Epron, J. Environ. Chem. Eng. (2015).
[35] S. Zuo, R. Zhou, Microporous Mesoporous Mater. 113 (2008) 472–480.
[36] M.A. Aramendía, V. Boráu, I.M. García, C. Jiménez, A. Marinas, J.M. Marinas, F.J. Urbano, Appl. Catal. B: Environ. 43 (2003) 71–79.
[37] K.L.E. Kaiser, V.S. Palabrica, Water Pollut. Res. J. Can. 26 (1991) 361–431.
[38] A.M. Polo, M. Tobajas, S. Sanchis, A.F. Mohedano, J.J. Rodriguez, Biodegradation 22 (2011) 751–761.
[39] V.M. Monsalvo, A.F. Mohedano, J.A. Casas, J.J. Rodriguez, Bioresour. Technol. 100 (2009) 4572–4578.
[40] A.H. Pizarro, V.M. Monsalvo, C.B. Molina, A.F. Mohedano, J.J. Rodriguez, Chem. Eng. J. 273 (2015) 363–370.